columns placed on one of the core's principal bending axes and located on opposite sides of the shear center. By the use of a transition mechanism, multisection cores with changing locations of shear center can be analyzed. The model is useful for representing simply a complex core that is part of a larger structure.

The most concise model for the computer analysis of a core is the single warping column model. This consists of a vertical stack of column elements, each of whose usual six degrees of freedom per node has been augmented by a seventh, warping, degree of freedom. The warping column model, however, cannot be analyzed by a standard frame analysis program unless a special subroutine, to introduce the additional warping degree of freedom, is incorporated. Also, the warping column model cannot be used to represent multisectional cores because there is no mechanism to represent the changes of section, as is available for the two-column model.

REFERENCES

13.1 Kollbrunner, C.F. and Basler, K. *Torsion in Structures, An Engineering Approach.* Springer-Verlag, New York, 1969.

13.2 Umanskii, A.A. "Torsion and Bending of Thin-Walled Aircraft Structures" (in Russian). *Oborongiz* 1939.

13.3 Timoshenko, S.P. "Theory of Bending, Torsion and Buckling of Thin-Walled Members of Open Cross-Section." *J. Franklin Inst.* **239,** March, April, May 1945, 201–219, 249–268, 343–361, respectively.

13.4 Vlasov, V.Z. *Thin-Walled Elastic Beams*, 2nd ed. (translated from the Russian by the Israel Program for Scientific Translations for the N.S.F. and Department of Commerce, U.S.A.). Office of Technical Services, Washington, D.C., 1961.

13.5 Stafford Smith, B. and Taranath, B.S. "Analysis of Tall Core-Supported Structures Subject to Torsion." *Proc. Inst. Civ. Engineers.* **53,** September 1972, 173–187.

13.6 Heidebrecht, A.C. and Stafford Smith, B. "Approximate Analysis of Open-Section Shear Walls Subject to Torsional Loading." *Proc. ASCE* ST12, December 1973, 2355–2373.

13.7 Stafford Smith, B. and Jesien, W. "Two-Column Model for Static Analysis of Mono-Symmetrical Thin-Walled Beams." *Structural Engineering Report No. 88-3.* Department of Civil Engineering and Applied Mechanics, McGill University, May 1988.

13.8 Weaver, W.J., Brandow, G.E., and Manning, T.A. "Tier Buildings with Shear Cores, Bracing and Setbacks." *Computers Structures* **1,** 1971, 57–83.

CHAPTER 14

Outrigger-Braced Structures

An outrigger-braced high-rise structure consists of a reinforced-concrete or braced steel frame main core connected to the exterior columns by flexurally stiff horizontal cantilevers. The core may be located between the column lines with outriggers extending on both sides (Fig. 14.1a) or it may be located on one side of the building with cantilevers connecting to columns on the other side (Fig. 14.1b).

When horizontal loading acts on the building, the column-restrained outriggers resist the rotation of the core, causing the lateral deflections and moments in the core to be smaller than if the free-standing core alone resisted the loading (Fig. 14.2a, b, and c). The result is to increase the effective depth of the structure when it flexes as a vertical cantilever, by inducing tension in the windward columns and compression in the leeward columns.

In addition to those columns located at the ends of the outriggers, it is usual to also mobilize other peripheral columns to assist in restraining the outriggers. This is achieved by including a deep spandrel girder, or "belt," around the structure at the levels of the outriggers, as in Fig. 14.3; hence, the occasionally used name, "belt-braced structure."

To make the outriggers and belt girder adequately stiff in flexure and shear, they are made at least one, and often two, stories deep. Consequently, to minimize the obstruction they cause, they are usually located at plant levels.

A building can be stiffened effectively by a single level of outriggers at the top of the structure, in which case it is sometimes referred to as a "top-hat" structure. Each additional level of outriggers increases the lateral stiffness, but by a smaller amount than the previous additional level. Up to four outrigger levels may be used in very tall buildings.

While the outrigger system is very effective in increasing the structure's flexural stiffness, it does not increase its resistance to shear, which has to be carried mainly by the core.

In this chapter an approximate method of analysis [14.1, 14.2] is presented for uniform outrigger structures, that is, structures with a uniform core, uniform columns, and similar-sized outriggers at each level. Although practical structures differ significantly from the uniform structure, in having vertical members that reduce in size up the height, the method of analysis is useful in allowing a rough estimate of the deflections and forces for use in a preliminary design. This approximate method of analysis is also useful in providing an estimate of the optimum levels

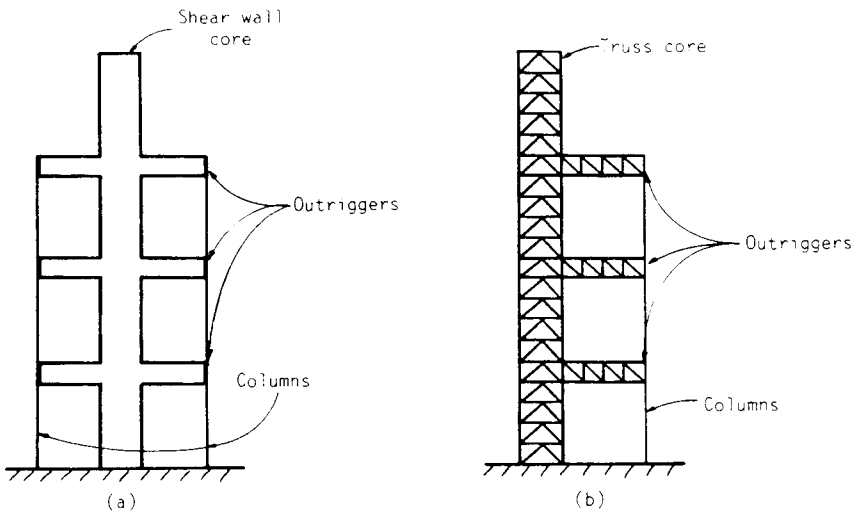

Fig. 14.1 (a) Outrigger structure with central core; (b) outrigger structure with offset core.

of the outriggers for minimizing the drift. The information provides guidance for the general arrangement of the structure.

14.1 METHOD OF ANALYSIS

Approximate methods of analysis for other types of high-rise structures, such as coupled walls and wall–frames, have been able to take advantage of the repetitive story-to-story arrangement in adopting a continuum approach. The outrigger-braced structure, with at most four outriggers, is not strictly amenable to a continuum analysis and has to be considered in its discrete arrangement. A compatibility method is chosen, in which the rotations of the core at the outrigger levels are matched with the rotations of the corresponding outriggers.

14.1.1 Assumptions for Analysis

The method of analysis is based on the following assumptions:

1. The structure is linearly elastic.
2. Only axial forces are induced in the columns.
3. The outriggers are rigidly attached to the core and the core is rigidly attached to the foundation.
4. The sectional properties of the core, columns, and outriggers are uniform throughout their height.

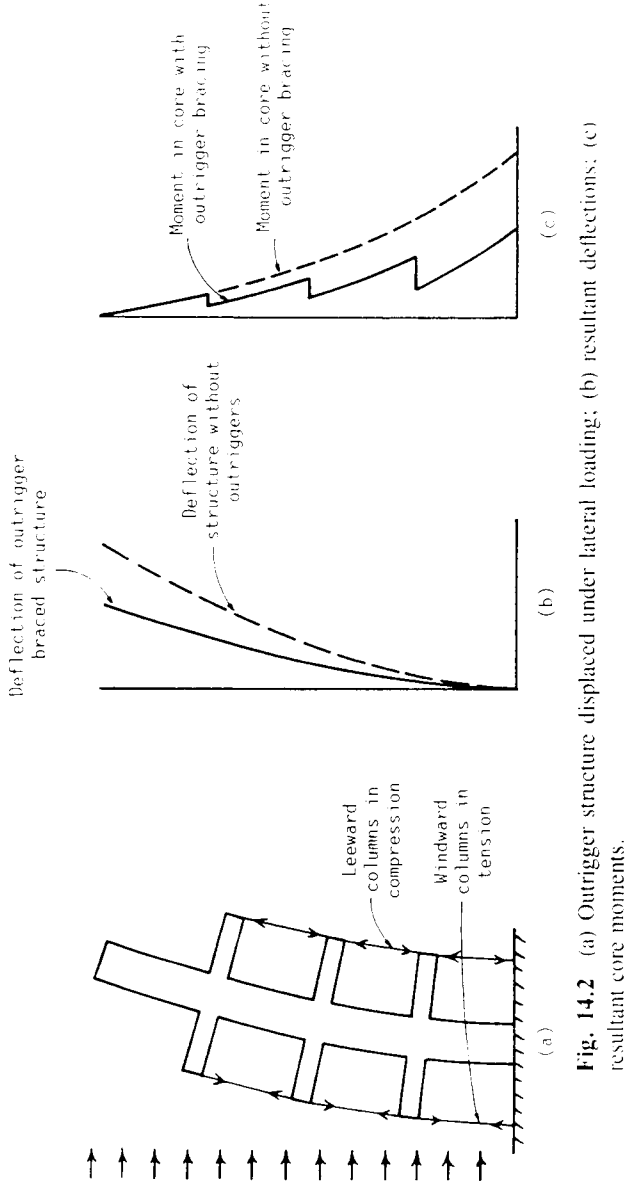

Fig. 14.2 (a) Outrigger structure displaced under lateral loading; (b) resultant deflections; (c) resultant core moments.

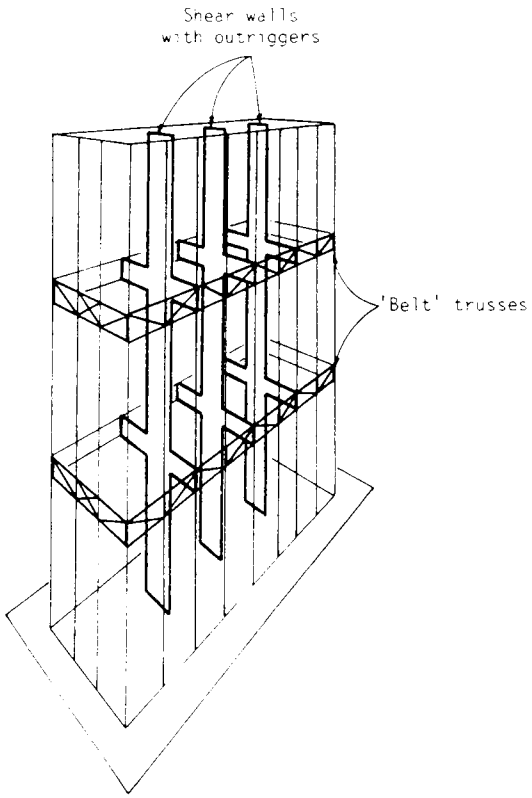

Fig. 14.3 Outrigger structure with belt girders.

Assumption 4 is less restrictive than at first it might appear. Although in a practical structure there is a reduction up the height in the inertia of the core and the sectional area of the columns, the factors of concern in a preliminary analysis (i.e., the drift at the top, the moment at the base of the core, and axial forces in the columns) are predominantly influenced by the properties of the structure in the lowest region. Consequently, an analysis of a uniform structure, with the "lowest region" properties of the actual structure, will give results of sufficient accuracy for a preliminary design.

14.1.2 Compatibility Analysis of a Two-Outrigger Structure

A two-outrigger structure will be used to demonstrate the method of analysis because it includes all the necessary steps in their simplest form. The analysis of structures with more or fewer than two outriggers can then easily be performed on the basis of the method for the two-outrigger case.

Starting from the statically determinate free standing core, a one outrigger structure is once redundant, a two outrigger structure twice redundant, and so on.

The number of compatibility equations necessary for a solution corresponds to the degree of redundancy. The compatibility equations state, for each outrigger level, the equivalence of the rotation of the core to the rotation of the outrigger. The rotation of the core is expressed in terms of its bending deformation, and that of the outrigger in terms of the axial deformations of the columns and the bending of the outrigger.

The model for analysis is the two-outrigger structure shown in Fig. 14.4a, subjected to a uniformly distributed horizontal load. Two other loading cases have been studied, and some of their results will be summarized at the end of the chapter.

The bending moment diagram for the core (Fig. 14.4e) consists of the external load moment diagram (Fig. 14.4b) reduced by the outrigger restraining moments that, for each outrigger, are introduced at the outrigger level and extend uniformly down to the base (Fig. 14.4c and d).

From the moment-area method, the core rotations at levels 1 and 2 (Fig. 14.4a) are, respectively,

$$\theta_1 = \frac{1}{EI}\int_{x_1}^{x_2}\left(\frac{wx^2}{2} - M_1\right)dx + \frac{1}{EI}\int_{x_2}^{H}\left(\frac{wx^2}{2} - M_1 - M_2\right)dx \quad (14.1)$$

and

$$\theta_2 = \frac{1}{EI}\int_{x_2}^{H}\left(\frac{wx^2}{2} - M_1 - M_2\right)dx \quad (14.2)$$

in which EI and H are the flexural rigidity and total height of the core, w is the intensity of horizontal loading, x_1 and x_2 are the respective heights of outriggers 1 and 2 from the top of the core, and M_1 and M_2 are their respective restraining moments on the core.

Expressions for the rotations of the outriggers at the points where they are connected to the core (i.e., at the "inboard" ends) will now be developed. Each rotation consists of two components: one allowed by the differential axial deformations of the columns, and the other by the outriggers bending under the action of the column forces at their "outboard" ends.

The rotation of the "inboard" ends of the outrigger at level 1 is

$$\theta_1 = \frac{2M_1(H - x_1)}{d^2(EA)_c} + \frac{2M_2(H - x_2)}{d^2(EA)_c} + \frac{M_1 d}{12(EI)_0} \quad (14.3)$$

and for the outrigger at level 2

$$\theta_2 = \frac{2(M_1 + M_2)(H - x_2)}{d^2(EA)_c} + \frac{M_2 d}{12(EI)_0} \quad (14.4)$$

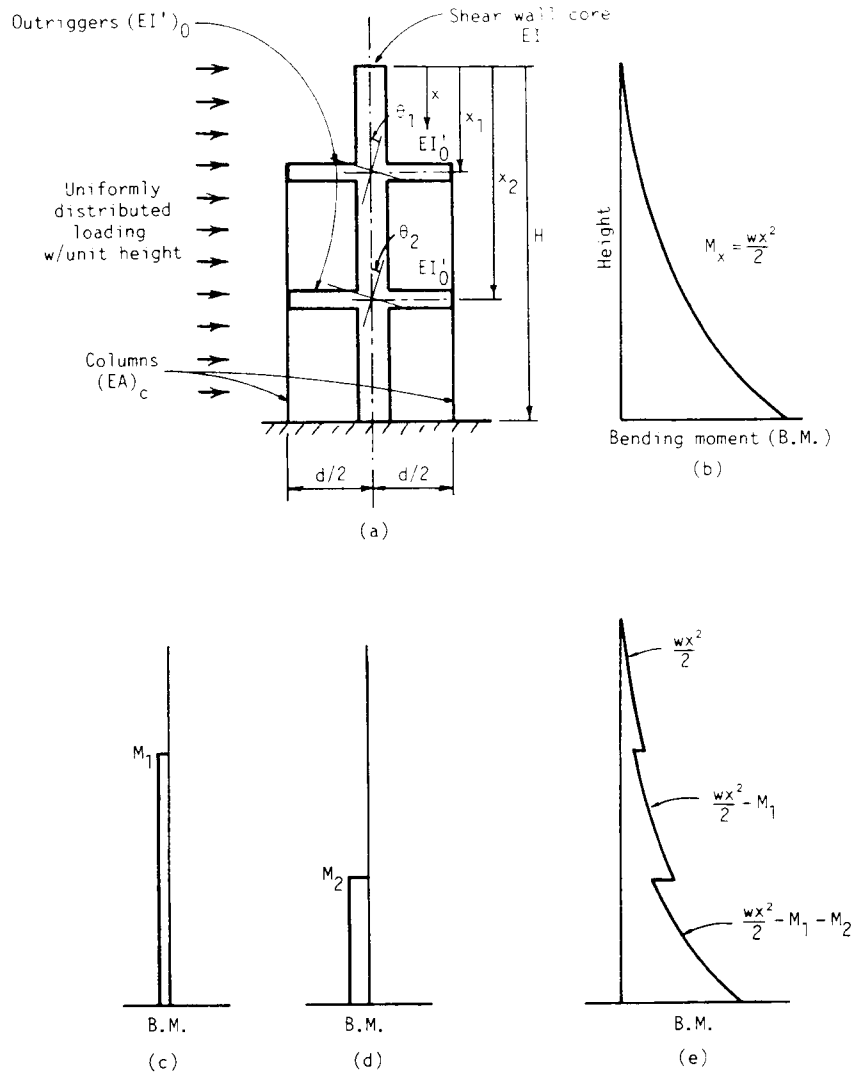

Fig. 14.4 (a) Two-outrigger structure; (b) external moment diagram; (c) M_1 diagram; (d) M_2 diagram; (e) core resultant moment diagram.

in which $(EA)_c$ is the axial rigidity of the column and $d/2$ is its horizontal distance from the centroid of the core. $(EI)_0$ is the effective flexural rigidity of the outrigger (Fig. 14.5b), allowing for the wide-column effect of the core, which can be obtained from the actual flexural rigidity of the outrigger $(EI')_0$ (Fig. 14.5a) as

$$(EI)_0 = \left(1 + \frac{a}{b}\right)^2 (EI')_0 \qquad (14.5)$$

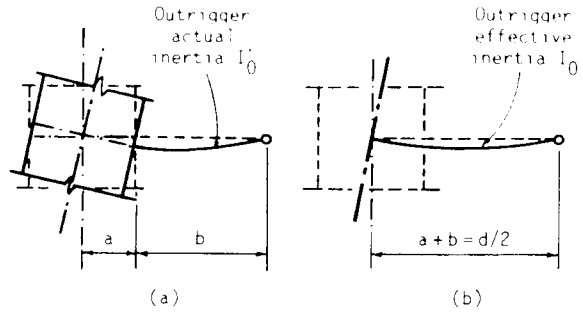

Fig. 14.5 (a) Outrigger attached to edge of core; (b) equivalent outrigger beam attached to centroid of core.

Equating the rotations of the core and outrigger at level 1, Eqs. (14.1) and (14.3), respectively

$$\frac{2M_1(H - x_1)}{d^2(EA)_c} + \frac{2M_2(H - x_2)}{d^2(EA)_c} + \frac{M_1 d}{12(EI)_0} = \frac{1}{EI}\left[\int_{x_1}^{x_2}\left(\frac{wx^2}{2} - M_1\right)dx + \int_{x_2}^{H}\left(\frac{wx^2}{2} - M_1 - M_2\right)dx\right] \qquad (14.6)$$

and similarly for the rotations at level 2, equating Eqs. (14.2) and (14.4),

$$\frac{2(M_1 + M_2)(H - x_2)}{d^2(EA)_c} + \frac{M_2 d}{12(EI)_0} = \frac{1}{EI}\int_{x_2}^{H}\left(\frac{wx^2}{2} - M_1 - M_2\right)dx \qquad (14.7)$$

Rewriting Eqs. (14.6) and (14.7) gives

$$M_1[S_1 + S(H - x_1)] + M_2 S(H - x_2) = \frac{w}{6EI}(H^3 - x_1^3) \qquad (14.8)$$

and

$$M_1 S(H - x_2) + M_2[S_1 + S(H - x_2)] = \frac{w}{6EI}(H^3 - x_2^3) \qquad (14.9)$$

in which S and S_1 are

$$S = \frac{1}{EI} + \frac{2}{d^2(EA)_c} \qquad (14.10)$$

$$S_1 = \frac{d}{12(EI)_0} \qquad (14.11)$$

14.1.3 Analysis of Forces

The simultaneous solution of Eqs. (14.8) and (14.9) gives the restraining moment applied to the core by the outrigger at level 1

$$M_1 = \frac{w}{6EI}\left|\frac{S_1(H^3 - x_1^3) + S(H - x_2)(x_2^3 - x_1^3)}{S_1^2 + S_1S(2H - x_1 - x_2) + S^2(H - x_2)(x_2 - x_1)}\right| \tag{14.12}$$

and, for the moment applied to the core by the outrigger at level 2,

$$M_2 = \frac{w}{6EI}\left|\frac{S_1(H^3 - x_2^3) + S\left[(H - x_1)(H^3 - x_2^3) - (H - x_2)(H^3 - x_1^3)\right]}{S_1^2 + S_1S(2H - x_1 - x_2) + S^2(H - x_2)(x_2 - x_1)}\right| \tag{14.13}$$

Having solved the outrigger restraining moments M_1 and M_2, the resulting moment in the core, which is shown in Fig. 14.4e, can be expressed generally by

$$M_x = \frac{wx^2}{2} - M_1 - M_2 \tag{14.14}$$

in which M_1 is included only for $x > x_1$, and M_2 is included only for $x > x_2$.

The forces in the columns due to the outrigger action are $\pm M_1/d$ for $x_1 < x < x_2$ and $(M_1 + M_2)/d$ for $x \geq x_2$.

The maximum moment in the outriggers is then $M_1 \cdot b/d$ for level 1 and $M_2 \cdot b/d$ for level 2, where b is the net length of the outrigger (Fig. 14.4a).

14.1.4 Analysis of Horizontal Deflections

The horizontal deflections of the structure may be determined from the resulting bending moment diagram for the core by using the moment-area method. A general expression for deflections throughout the height could be written; it would, however, be very complicated. Concentrating, therefore, on the top drift only, this may be expressed as

$$\Delta_0 = \frac{wH^4}{8EI} - \frac{1}{2EI}\left[M_1(H^2 - x_1^2) + M_2(H^2 - x_2^2)\right] \tag{14.15}$$

in which the first term on the right-hand side represents the top drift of the core acting as a free vertical cantilever subjected to the full external loading, while the two parts of the second term represent the reductions in the top drift due to the outrigger restraining moments M_1 and M_2.

14.2 GENERALIZED SOLUTIONS OF FORCES AND DEFLECTIONS

So far, the method of analysis of only a two-outrigger structure has been presented. The same method of analysis applied to structures with more, or fewer, than two outriggers leads to expressions for restraining moments and top drift having the same form as Eqs. (14.14) and (14.15), respectively. By induction from these, generalized expressions may be developed, as follows.

14.2.1 Restraining Moments

The restraining moments for a uniform structure subjected to uniformly distributed loading may be expressed concisely in matrix form for simultaneous solution by computer:

$$\begin{bmatrix} M_1 \\ M_2 \\ \vdots \\ M_i \\ \vdots \\ M_n \end{bmatrix} = \frac{w}{6EI} \cdot \begin{bmatrix} S_1 + S(X - X_1) & S(H - X_2) & \cdots & S(H - X_i) & \cdots & S(H - X_n) \\ S(H - X_2) & S_1 + S(H - X_2) & \cdots & S(H - X_i) & \cdots & S(H - X_n) \\ \vdots & \vdots & \vdots & \vdots & \vdots & \vdots \\ S(H - X_i) & S(H - X_i) & \cdots & S_1 + S(H - X_i) & \cdots & S(H - X_n) \\ \vdots & \vdots & \vdots & \vdots & \vdots & \vdots \\ S(H - X_n) & S(H - X_n) & \cdots & S(H - X_n) & \cdots & S_1 + S(H - X_n) \end{bmatrix} \cdot \begin{bmatrix} H^3 - X_1^3 \\ H^3 - X_2^3 \\ \vdots \\ H^3 - X_i^3 \\ \vdots \\ H^3 - X_n^3 \end{bmatrix} \tag{14.16}$$

in which n is the number of levels of outriggers. Equation (14.16) requires that the properties of the structure, the levels of the outriggers, and the magnitude of loading be specified.

A general expression for the moment in the core between outriggers j and $j + 1$ is then

$$M_x = \frac{wx^2}{2} - \sum_{i=1}^{j} M_i \tag{14.17}$$

In the region between the top of the structure and the first outrigger from the top, the second term on the right-hand side of Eq. (14.17) will be zero.

14.2.2 Horizontal Deflections

Substitution of restraining moments M_1 to M_n, from the solution of Eq. (14.16) into Eq. (14.18) gives the resultant deflection at the top of the structure.

$$\Delta_0 = \frac{wH^4}{8EI} - \frac{1}{2EI} \sum_{i=1}^{n} M_i (H^2 - x_i^2) \tag{14.18}$$

14.3 OPTIMUM LOCATIONS OF OUTRIGGERS

The preceding analysis is useful in not only providing estimates of the core moments and horizontal deflections, but also allowing an assessment of the optimum levels of the outriggers to minimize the horizontal top deflection. This is achieved by maximizing the drift reduction [i.e., the second term on the right-hand side of Eq. (14.18)].

Illustrating the procedure by continuing to consider the two-outrigger structure, the second term of its deflection equation [Eq. (14.15)] is maximized by differentiating with respect first to x_1, then to x_2, thus

$$(H^2 - x_1^2)\frac{dM_1}{dx_1} + (H^2 - x_2^2)\frac{dM_2}{dx_1} - 2x_1M_1 = 0 \tag{14.19}$$

and

$$(H^2 - x_1^2)\frac{dM_1}{dx_2} + (H^2 - x_2^2)\frac{dM_2}{dx_2} - 2x_2M_2 = 0 \tag{14.20}$$

in which dM_1/dx_1, dM_2/dx_1, dM_1/dx_2, and dM_2/dx_2 are the derivatives of M_1 and M_2 from Eqs. (14.12) and (14.13), respectively, with respect to x_1 and x_2. Substituting for M_1 and M_2 and their derivatives, Eqs. (14.19) and (14.20) can be solved simultaneously for the values of x_1 and x_2 that define the optimum levels of the outriggers. The solution of Eqs. (14.19) and (14.20) is, obviously, complex; therefore, a numerical method of solution by computer is necessary.

In the complete expressions for Eqs. (14.19) and (14.20), the structural properties were expressed initially by parameters S and S_1, as defined by Eqs. (14.10) and (14.11). Equations (14.19) and (14.20) can be rewritten in terms of more meaningful nondimensional parameters α and β, which represent the core to column and core-to-outrigger rigidities, respectively, as follow

$$\alpha = \frac{EI}{(EA)_c(d^2/2)} \tag{14.21}$$

and

$$\beta = \frac{EI}{(EI)_0}\frac{d}{H} \tag{14.22}$$

It is then possible to simplify Eqs. (14.19) and (14.20) further by combining α and β into a single parameter ω, as defined by

$$\omega = \frac{\beta}{12(1 + \alpha)} \tag{14.23}$$

The parameter ω, which is nondimensional, is the characteristic structural parameter for a uniform structure with flexible outriggers. It is useful in that it allows various aspects of the behavior of outrigger structures to be expressed in a very concise form.

It may be deduced from Eqs. (14.21) to (14.23) that, with all other properties remaining constant, there is a reduction in ω as the outriggers' flexural stiffnesses are increased, and that ω increases as the axial stiffnesses of the columns increase.

Equations (14.19) and (14.20) may be solved to find the optimum outrigger levels, 1 and 2, for a range of values of ω, to give the results plotted graphically in Fig. 14.6b. Thus, for any uniform two-outrigger structure having specified member properties, ω may be calculated and Fig. 14.6b used to determine the optimum locations for the outriggers in order to achieve minimum drift.

The described procedure leading to the results plotted in Fig. 14.6b for a two outrigger structure has been repeated for one-, three-, and four-outrigger structures. The graphs showing the optimum outrigger locations are given in Fig. 14.6a, c, and d, respectively.

14.4 PERFORMANCE OF OUTRIGGER STRUCTURES

Although the method of analysis for uniform structures presented earlier is useful in estimating the forces and drift for preliminary design, it is of further value in providing general information about the most efficient arrangement of the structure. This guidance relates particularly to the appropriate number and location of the outriggers, as follows

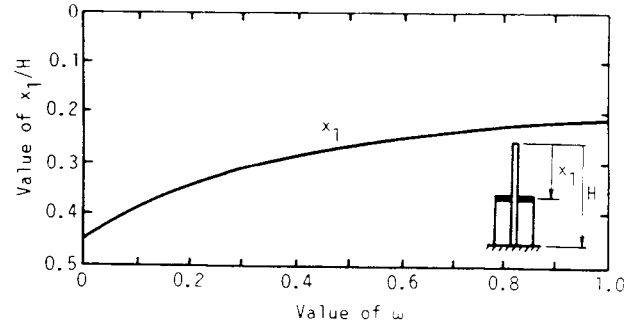

(a)

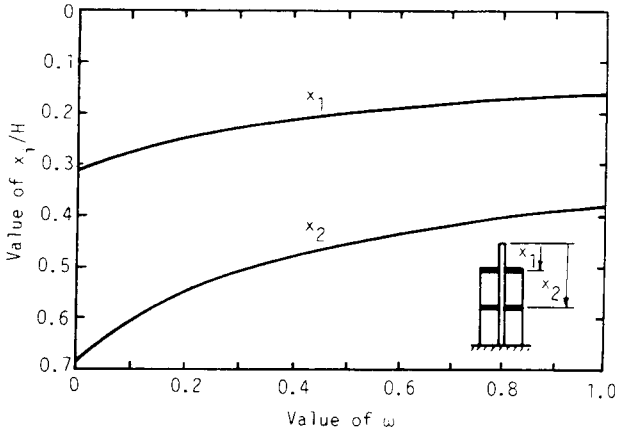

(b)

Fig. 14.6 (a) Optimum outrigger location for one-outrigger structure; (b) optimum outrigger locations for two-outrigger structure.

14.4.1 Optimum Locations of Outriggers

Considering, for purposes of comparison, hypothetical structures in which the outriggers are flexurally rigid (i.e., with ω equal to zero) the curves in Fig. 14.6a–d may be interpreted to yield simple approximate guidelines for the location of the outriggers to minimize the deflection: the outrigger in a one-outrigger structure should be at approximately half-height; the outriggers in a two-outrigger structure should be at approximately one-third and two-thirds heights; in a three outrigger structure they should be at approximately the one-quarter, one-half, and three quarters heights, and so on. Generally, therefore, for the optimum performance of an n-outrigger structure, the outriggers should be placed at the $1/(n+1)$, $2/(n+1)$, up to the $n/(n+1)$ height locations.

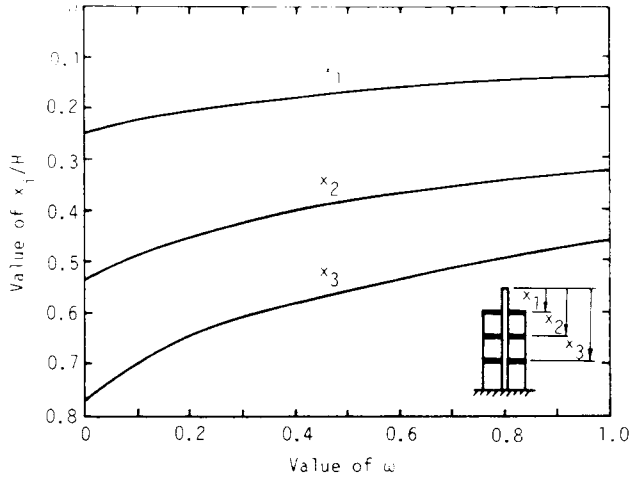

(c)

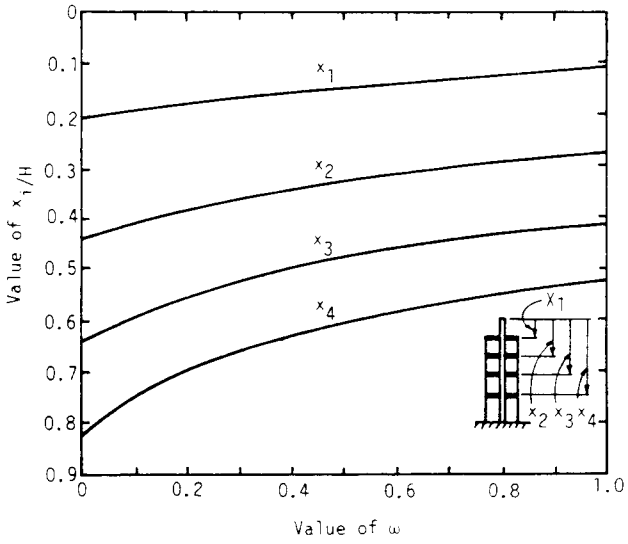

(d)

Fig. 14.6 *(Continued)* (c) Optimum outrigger locations for three-outrigger structure; (d) optimum outrigger locations for four-outrigger structures.

In any outrigger system it is, perhaps unexpectedly, structurally inefficient to locate an outrigger at the top, and it should only be done when other reasons (e.g., a plant floor located at the top) prevail.

Indeed, it has been shown [14.1] that a structure with n optimally located outriggers is almost as effective in its lateral resistance as the same structure with an

additional outrigger at the top. In a uniform structure, the lowest outrigger always induces the maximum restraining moment, with the outriggers above carrying successively less. In an optimally arranged structure, the moment carried by an outrigger ranges from one-half to two-thirds that carried by the outrigger below. However, in an optimally arranged structure, but with an additional outrigger at the top, the top outrigger carries approximately one-sixth of the moment of the outrigger below. This illustrates clearly the inefficiency of including a top outrigger.

14.4.2 Effects of Outrigger Flexibility

In real structures, the flexibility of the outriggers makes it necessary to modify the above guidelines. The curves in Fig. 14.6a–d show that the larger the value of ω (i.e., the more flexible the outriggers) the further up the structure the set of outriggers must be located in order to minimize the drift. The relative intervals between the outriggers and the top, however, remain approximately the same.

14.4.3 "Efficiency" of Outrigger Structures

A useful measure of the effectiveness of an outrigger system in reducing the free-standing core's lateral deflection and base moment is to express the resulting reductions as percentages of the corresponding reductions that would occur if the core and columns behaved fully compositely. Fully composite action implies that, in overall flexure of the structure, the stresses in the vertical components are proportional to their distances from their common centroidal axis, with the structure having an overall flexural rigidity equal to

$$(EI)_t = \frac{(EA)_c\, d^2}{2} + EI \qquad (14.24)$$

It has been shown [14.2] that the percentage efficiencies for both drift and base moment reductions can be expressed in terms of ω. These are plotted for one- to four-outrigger structures in Fig. 14.7a and b, respectively.

Considering the one-outrigger structure with a flexurally rigid outrigger, the maximum efficiency in drift reduction is 87.5%, and the corresponding efficiency in core base moment reduction is 58.3%. For two-, three-, and four-outrigger structures, the respective efficiencies are 95.5%, 70.3%; 97.8%, 77.1%; and 98.5%, 81.3%. Evidently, for structures with very stiff outriggers (i.e., with low values of ω) there is little to be gained in drift control by exceeding four outriggers, hence the reason for the graphs being plotted for up to only four outriggers.

The optimum outrigger arrangement for the maximum reduction in drift does not simultaneously cause the maximum reduction in the core base moment. For this, the outriggers would have to be lowered toward the base.

In cases where drift control is not critical, the design emphasis could change to controlling the core moments by lowering the levels of the outriggers until the drift limitations are just satisfied. Such a refined consideration of the structure is rarely

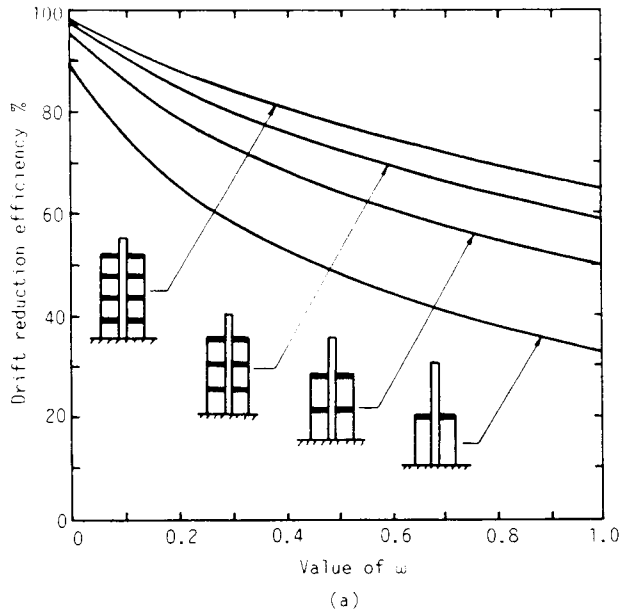

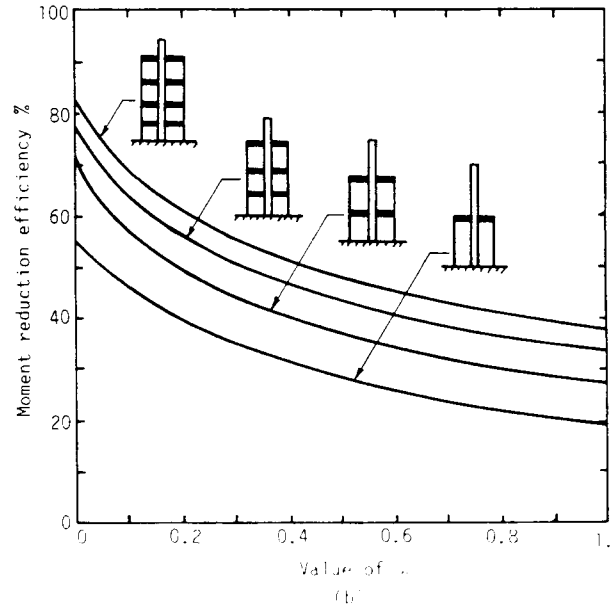

Fig. 14.7 (a) Efficiency in drift reduction, (b) efficiency in moment reduction

possible in practice. However, the designer's general appreciation of how various factors influence the performance of an outrigger structure should lead to his making a better choice when alternative outrigger arrangements are possible.

14.4.4 Alternative Loading Conditions

Analysis of outrigger braced structures subjected to a triangular load distribution, with its apex at the base, and a concentrated top load have also been made. These are useful for considering graduated wind loading and static equivalent earthquake loading. [14.3].

It was deduced that the "minimum top drift" optimum levels of the outriggers for the triangular loading were only slightly higher than those deduced for uniformly distributed loading. The optimum levels for the concentrated top load were slightly higher than those for the triangularly distributed loading.

Considering that wind loading distributions are usually in the form of a trapezium, consisting of superposed uniform and triangular loading distributions, and the static equivalent earthquake loading is usually given as a triangular distribution with a relatively small concentrated load at the top, it may be concluded from the above observations that the "minimum top drift" optimum levels may reasonably be taken as approximately those obtained for uniformly distributed loading.

SUMMARY

A compatibility method of analysis for the forces and deflections in uniform outrigger-braced structures subjected to uniformly distributed lateral loading is presented. Taking as an example a two-outrigger structure, the rotation of the core at each outrigger level (derived from the distribution of moments in the core) is matched with the rotation of the "inboard" end of the corresponding outrigger (derived from the axial deformation of the columns and the flexure of the outrigger). The resulting compatibility equations are solved to give the outrigger restraining moments. From these, the core moment diagram, the outrigger moments, and the column axial forces may be determined. The horizontal deflections of the structure are then obtained from the core moment diagram by, for example, the moment-area method.

The method of analysis presented for a two-outrigger structure can be extended to structures with other numbers of outriggers, leading by induction to generalized equations for the restraining moments and horizontal displacements.

Optimum levels of the outriggers for minimum top drift are obtained by maximizing the drift reduction caused by the outriggers. These are plotted as a function of a nondimensional relative stiffness parameter ω, for structures with up to four outriggers and with variable stiffnesses of the core and outrigger system. The efficiencies of uniform-with-height outrigger structures are assessed with regard to drift and core base moment reductions. These are plotted as functions of ω for

structures with one to four outriggers, and for outrigger systems of varying stiffness properties.

The optimum levels of outriggers for the minimum drift of structures subjected to a triangularly distributed load, with its apex at the base, are slightly higher than for structures subjected to a uniformly distributed load, while the optimum levels in structures subjected to a concentrated top load are slightly higher again.

REFERENCES

14.1 Stafford Smith, B. and Nwaka, I. O. "Behavior of Multioutrigger Braced Tall Buildings." *ACI Special Publication SP-63*, 1980, 515–541.

14.2 Stafford Smith, B. and Salim, I. "Parameter Study of Outrigger-Braced Tall Building Structures." *Proc. ASCE* **107**, ST10, October 1981, 2001–2014.

14.3 Coull, A. and Lau, W. H. O. "Outrigger-Braced Structures Subjected to Equivalent Static Seismic Loading." *Proc. 4th Int. Conf. on Tall Buildings*, Hong Kong and Shanghai, Y. K. Cheung and P. K. K. Lee (Eds.), Vol. 1, Hong Kong, 1988, pp. 395–401.